Int. J. Rock Mech. & Min. Sci. Vol. 34, No. 3-4, 1997 ISSN 0148-9062
To cite this paper: *Int. J. Rock Mech. & Min. Sci.* **34:3–4**, Paper No. 190

CREEP AND STATIC FATIGUE OF WELDED TUFF FROM YUCCA MOUNTAIN, NEVADA

R. J. Martin[1]; J. S. Noel[1]; P. J. Boyd[1]; R. H. Price[2]

[1] **NEW ENGLAND RESEARCH, INC. 76 OLCOTT DRIVE, WHITE RIVER JUNCTION, VT 05001,** USA

[2] **SANDIA NATIONAL LABORATORIES ALBUQUERQUE, NEW MEXICO 87185**

ABSTRACT

Sixteen creep experiments were performed on welded tuff specimens from the vicinity of Yucca Mountain, NV. The tests were performed under two conditions. One suite of measurements was performed on nominally dry specimens at a confining pressure of 10 MPa, a temperature of 225 °C, and differential stresses between 40 and 130 MPa. The second suite of experiments was conducted on water saturated specimens at a confining pressure of 5.0 MPa, a pore pressure of 1.0 MPa, and a temperature of 150 °C over a range of differential stresses from 115 to 150 MPa. Six of the specimens tested at 150 °C failed in shear. The remaining experiments were terminated after 10^6 seconds prior to failure. All of the specimens tested showed primary and secondary stages of creep. The secondary creep strain increased as the differential stress was increased. The specimens that failed exhibited a tertiary creep stage. The specimens brought to failure were analyzed in terms of static fatigue. Based on limited data, the time to failure, $\langle t \rangle$, is given by an expression of the form

$$\langle t \rangle = 10^{41} e^{-0.646 \sigma}$$

where σ is the differential stress applied to the specimen.

KEYWORDS

Creep • static fatigue • stress corrosion cracking • brittle failure • radioactive waste isolation • strength • laboratory test

INTRODUCTION

Site characterization for the potential high level nuclear waste isolation facility at Yucca Mountain, NV is well underway. If the site characterization phase is successful, the site will be nominated to the President, and a license application filed with the Nuclear Regulatory Commission by the Department of Energy. The procedures leading to the selection and licensing are controlled by the nuclear waste isolation act of 1982. In 1987, the act was amended and Yucca Mountain was designated as the primary site for characterization and evaluation. If the site is deemed unsuitable by the Secretary of DOE, the site characterization will be terminated and other sites will be considered. A repository design will accompany the license application and will be developed on specific characteristics of data developed during the site characterization phases of the study.

An integral part of the site characterization is a comprehensive suite of laboratory measurements to determine the elastic, strength, thermal, electrical, and flow properties of the tuffs at Yucca Mountain. Many of these studies are well underway and have reached significant milestones. In this study we are concerned with the time dependent strength of tuffs in the potential repository horizon as a function of saturation, temperature, confining pressure, and differential stress. With the emplacement of waste the temperature of the rock mass in the vicinity of the repository will rise. Depending on the final design of the emplacement of canisters, the temperature of the potential repository may rise as high as 250 °C locally. Thermal stresses will develop during the heating. The thermal stresses coupled with the *in situ* tectonic stresses will cause the rocks in the vicinity of the emplacement horizon to deform.

Hardy , Bauer 1992 estimated that the greatest principal compressive stress due to these effects will approach 20 MPa ten years after the emplacement of the canisters. The exact value will depend on the canister density within the repository. To complete the performance assessment of the potential repository, it is prudent to determine the magnitude of the strain developed due to thermal loading and to determine whether or not the rocks will fail as the result of the increased stress. The design life of the proposed repository is ten thousand years. Consequently, we are looking at the time to failure for rock thermally loaded to temperatures of several hundred degrees centigrade under stress conditions that will exist in the repository due to thermal and tectonic stresses. In light of these considerations, a study has been undertaken to evaluate the time dependent deformation of tuff at elevated temperatures for two water saturations, and to examine the effect of these parameters on the long term strength of the rock mass in the vicinity of the emplacement canisters.

BACKGROUND

One of the most striking characteristics of brittle rocks is that at temperatures well below the melting point, a rock subjected to a constant load exhibits a continuous increase in strain with time. This time-dependent deformation is termed creep. Studies on creep indicate that the observed strain depends upon the applied stress, the temperature, the partial pressure of water, and the confining pressure (Matsushima 1960; Rummel 1969; Martin 1972b; Peng 1973; Kranz , Scholz 1977). Moreover, the same mechanism responsible for the strain of brittle rocks in constant strain-rate tests is also operative in creep. That is, cracking, both along grain boundaries and through individual grains, produces the observed strain (e.g., Brace *et al*. 1966; Scholz 1968; Wawersik 1972). Above approximately one half to two-thirds of the compressive strength, the dominant mode of deformation for brittle rocks is the opening and growth of axial cracks.

If time-dependent strains observed in brittle crystalline rocks are related to axial cracking, it might be asked, “Is there a basic time dependence associated with the formation and growth of axial cracks that may be related to creep?” One approach is to assume that axial cracks lengthen with time under a constant load and that the strain rate of rocks in creep is related to the time-dependent growth of these cracks.

Experimental results indicate that stable time-dependent crack-growth at a constant compressive load or at a constant stress intensity factor occurs in quartz and glass in the presence of water vapor. Moreover, the rate of crack growth depends on the applied stress, the temperature, and the partial pressure of water in the atmosphere surrounding the crack. The relative weakening of quartz or silicate glass, reflected by an increase in the rate of crack growth with an increase in any of the three variables, is consistent with the

ISSN 0148-9062

general theory of stress corrosion in silicates proposed by Charles 1965. He postulated that the velocity of a slowly propagating crack with a high tensile stress at the crack tip is proportional to the rate of the hydration reaction at the crack tip. Wiederhorn 1968 quantified the relationship with the following general equation for environment-sensitive crack growth

$$\nu = \nu_o \beta P^n \exp\left(\frac{\Delta F - V^* \sigma}{RT} + \frac{\gamma Vm}{\rho RT}\right) \quad (1)$$

where ν is the rate of crack growth, P is the partial pressure of water, ΔF is the activation energy for the process, T is temperature, R is the universal gas constant, V^* is the activation volume, σ is stress, γ is the surface energy of the solid, Vm is the molar volume of the solid, ρ is the radius of curvature of the crack tip, and β and n are constants.

If the partial pressure of water, the temperature, and the applied stress are constant, a constant crack propagation velocity will be observed. When any one of the thermodynamic variables is increased, the crack velocity increases. This expression has been verified with experimental studies (Wiederhorn 1968; Martin 1972a; Scholz 1972; Martin , Durham 1975; Dunning *et al*. 1978; Atkinson 1984).

Next, let us examine the behavior of brittle rocks during creep and then compare these observations with the results of stable, time-dependent crack growth. Typically, creep is reported in terms of three distinct phases: primary or transient creep, secondary or steady-state creep, and tertiary or accelerating creep.

Transient creep has been reported for a variety of rock types over a wide range of temperatures and pressures (Lomnitz 1956; Matsushima 1960, Misra , Murrell 1965; Rummel 1969; Kranz , Scholz 1977). The strain in this region decelerates rapidly and is often reported as proportional to the logarithm of time. Moreover, both the lateral and the longitudinal strains exhibit this logarithmic time dependence.

At low stresses, transient creep may account for the observed strain. However, at high stresses, secondary creep is often observed. Generally, in secondary creep, often called steady-state creep, the strain is proportional to time. The total strain caused by both primary and secondary creep is often represented by an equation of the form

$$\varepsilon = A + B \log t + Ct \quad (2)$$

where ε is strain, t is time, and A, B, and C are constants.

If secondary creep is allowed to continue, eventually the strain rate increases (tertiary creep) and the rock fails. All three stages of creep have been observed in granite, quartzite, diabase, and granodiorite (Lomnitz 1956; Matsushima 1960, Rummel 1969; Martin 1972a; Kranz , Scholz 1977).

Stable crack growth in quartz reported by Martin 1972a, Martin , Durham 1975, and Dunning *et al*. 1975 illustrated specific characteristics that are related to creep deformation. In these studies, the specimens were loaded to a fixed compressive stress and the growth of a crack parallel to the applied load was observed. The crack was initiated by drilling a small hole through the center of the specimen to act as a stress concentrator to initiate the crack. Each specimen was tested in a controlled environment and the change in crack length was noted as a function of time. A typical data set obtained on a single specimen of quartz tested at a temperature of 241 °C and a partial pressure of water of 4.5×10^{-2} kPa is shown in Figure 1. The test specimen geometry is shown in the upper left portion of the graph. At a stress of 66

ISSN 0148-9062

MPa, the change in crack length with time is very similar to that observed in the creep of brittle crystalline rocks. The crack exhibits an initial period of rapidly decelerating growth followed by a quasi-linear or secondary segment. After 6.3×10^4 seconds, the stress was increased to 74 MPa. Immediately, the rate of crack growth increased. The same characteristics observed at the lower stress were exhibited for the 74 MPa segment. There was a strong transient followed by a secondary or quasi-linear crack growth segment. At approximately 8×10^4 seconds, the stress was increased to 83 MPa. The rate of crack growth increased dramatically; the experiment was terminated when the crack length reached 3.7 mm. These data are consistent with Equation 1; that is, the rate of crack growth increased with increasing stress and nearly vanishes at low stresses. Additional experiments showed that increasing either the partial pressure of water surrounding the crack or the temperature also results in an increase in the rate of crack growth.

Equation 1 predicts crack growth at a constant velocity. This is not observed in the specimens tested where the applied load is compressive. Several reasons have been suggested to explain this behavior. First, the partial pressure of water at the crack tip decreases as the crack length increases. Propagation occurs when hydration reaction alters the covalent Si-O bonds to form weaker Si-OH Van der Waal type bonds. This reaction produces a volume increase, which reduces the diffusivity along the path to the crack tip. The net effect is a reduction of the partial pressure of water at the crack tip, which inhibits growth. Second, the stress intensity factor at the crack tip decreases with increasing crack length.

The similarity in form between the creep curve and that for time-dependent crack growth is not sufficient to conclude that crack growth is the mechanism of creep in brittle rocks. What is needed is a theory of creep that defines the observed strain in terms of time-dependent crack growth. Martin 1972a showed that for randomly oriented cracks, the strain-rate of a rock in creep is proportional to the rate of crack growth. If the only effect of increasing the temperature, stress, or partial pressure of water was to augment the rate of crack growth on pre-existing cracks, the same dependencies for an isolated crack in quartz should closely approximate those in brittle silicate rocks.

An alternative approach is to consider a model based on the time required for a crack to extend to a critical length and not consider the details of propagation. Scholz 1968 has demonstrated that creep can be treated statistically as the static fatigue of independent regions throughout the rock. Static fatigue refers to the failure time of a rock or single crystal at constant stress, temperature, confining pressure, and partial pressure of water without regard to the strain history. Scholz 1972 conducted a series of static fatigue tests in compression on single crystal quartz. He observed that the mean time to failure, $\langle t \rangle$, depended on the partial pressure of water, P; stress, σ; and temperature, T, according to

$$\langle t \rangle = t_o P^{-a} \exp \left(\frac{\Delta F}{RT} - K' \sigma \right) \qquad (3)$$

where a and K' are constants.

The foregoing discussion demonstrates that the strength of brittle, silicate rocks is not a single-valued function of any parameter, but is a complex continuum that depends on the state of stress, the saturation (pore pressure), the temperature, and the time (including strain rate).

Since the potential nuclear waste repository at Yucca Mountain will be subjected to uncommon conditions, it seems prudent to bound the creep behavior and long-term strength of the tuff. It will be of particular interest to know how the strength of tuff varies with time, temperature, stress, and saturation. If

ISSN 0148-9062

the repository is to experience temperatures in excess of 200 °C, the strength of the rock probably will be degraded. Furthermore, changes in saturation will have an impact on the strength. Finally, because the repository will experience thermally induced stresses for a significant portion of its design life, it is necessary to quantify the effect of this long-term loading on time-dependent deformation.

EXPERIMENTAL PROCEDURE FOR CREEP EXPERIMENTS AT ELEVATED TEMPERATURE AND PRESSURE

Sixteen specimens of welded tuff recovered from borehole NRG-7/7A at Yucca Mountain and from Busted Butte, adjacent to Yucca Mountain, were tested in triaxial creep as a function of temperature, confining pressure, pore pressure, and differential stress. Each specimen was tested for approximately 10^6 seconds or until the specimen failed. The welded tuff is characteristic of the proposed repository horizon. The tuff is a densely welded, devitrified, lithophysae pore unit of the Paintbrush tuff. The welded tuff is composed of shards, pumice, and matrix. Pumice is the major constituent; it occurs as elongated fragments compacted and flattened during welding. The porosity of the specimens ranged between 7.5 and 11.5 percent. The specimens from the borehole on Yucca Mountain were selected from available core from the depth of the potential repository horizon. The specimens prepared from boulders collected at Busted Butte were from the same block of rock and therefore their chemical composition, and lithophysae characteristics are more constant.

The creep experiments were performed on ground, right circular cylinders of TSw2 tuff 50.8 mm in diameter with a nominal length to diameter ratio of 2 to 1, as a function of confining pressure, temperature, and water saturation. The specimens are jacketed and inserted in a pressure vessel. The jacket consists of two layers of 0.13 mm thick soft copper wrapped around the specimen and extending 12 mm beyond the end of each specimen. Hardened steel end caps are then positioned at the end of the test specimens. The entire sample assembly is then jacketed with teflon heat shrink tubing and secured with wraps of wire. The confining pressure and temperature are increased to specified conditions. A differential stress is rapidly applied to the specimen (less than 10 seconds) and held constant for the duration of the test. The deformation of the specimen is measured as a function of time.

The specimens were tested under two conditions. The specimens recovered from borehole NRG-7/7A were tested drained and vented to the atmosphere at a temperature of 225 °C and a confining pressure of 10 MPa. The experiments were performed at stresses between 40 and 130 MPa. A drained and vented boundary condition is anticipated after the emplacement of waste at Yucca Mountain. Specifically, the temperature will increase, drying the rock mass to a constant, albeit low partial pressure of water. In contrast, the specimens prepared from boulders recovered at Busted Butte were tested at a confining pressure of 5 MPa, a pore water pressure of 1 MPa, and a temperature of 150 °C. The objective of these experiments was to observe the creep behavior for specimens taken to failure and to develop a constitutive law for the time to failure as a function of differential stress. Ultimately, we will test similar specimens at different water saturations and temperatures to completely define the static fatigue characteristics of the welded tuff for the potential repository horizon.

The creep measurements are conducted in a servo-hydraulic creep testing apparatus. The key features of the system include independent controls for the (1) axial force, producing the differential stress on the sample, (2) confining pressure, (3) pore pressure, and (4) temperature. The creep apparatus is a compact unit designed to handle test specimens up to 50.8 mm in diameter and 120 mm in length, at confining pressures to 35 MPa, pore pressures to 35 MPa, and temperatures to 225 °C. The system, as configured

ISSN 0148-9062

for these experiments, exerts a maximum axial force on the specimen of 640 kN.

A schematic diagram of the pressure vessel is shown in Figure 2. Since the apparatus design is specifically adapted to conduct creep measurements on specimens up to 50.8 mm in diameter, it is possible to use an extremely compact test apparatus. The system consists of a pressure vessel divided into two chambers separated with a moveable piston. The specimen resides in the low pressure chamber. This chamber exerts confining pressure on the specimen. The higher pressure, in the upper chamber, moves the piston in contact with the sample assembly. The force exerted on the sample is given by

$$F = P_a A_a - P_c A_c - f_s \qquad (4)$$

where P_c is the confining pressure, A_c is the area of the piston in the low pressure chamber, P_a is the pressure in the high pressure chamber, A_a is the effective area of the piston in the high pressure chamber, and f_s is the seal friction. With this system the confining pressure and differential stress are constant to ± 0.10 MPa during the creep experiments.

The vessel is heated with an external furnace. The furnace consists of three band heaters positioned on the outside of the pressure vessel to produce a uniform temperature distribution throughout the test specimen. The temperature gradient along the length of the sample deviated by less than 3 °C from end to end. The variation of temperature at the midpoint of the sample during a test is within ± 1 °C.

The axial strain of the specimen is measured with an external displacement transducer (LVDT). The displacement of the moveable piston inside the pressure vessel is measured with respect to the closure plug for the high pressure chamber of the pressure vessel. The displacement of the piston is continuously monitored throughout the experiment. Since the differential stress, confining pressure, pore pressure, and temperature remain constant throughout the experiment, the displacement observed as a function of time is directly related to the shortening of the specimen.

EXPERIMENTAL RESULTS

The data for sixteen creep experiments are reported. Six samples failed at times less than 2×10^6 seconds. The remainder of the specimens did not fail after a minimum of 10^6 seconds and the experiments were terminated. The results for four experiments are shown in Figures 3, 4, and 5. Three of these specimens failed. The tests were performed at a confining pressure of 5.0 MPa, a pore pressure of 1.0 MPa, and a temperature of 150 °C. The creep strain is plotted as a function of time for each experiment. We define creep strain as the time dependent strain that occurs after the specimen is loaded to 98% of the constant peak differential stress. Since loading in some cases took as long as ten seconds this point was arbitrarily selected as the onset of inelastic shortening of the specimen. The data show a consistent trend; a strong initial transient followed by quasi-linear secondary creep. Data on two of the specimens shown in Figures 3 and 4 displayed accelerating tertiary creep. The jitter in the creep strain versus time curve in Figure 5 are artifacts of the way in which the strain was measured. The LVDT is mounted outside the pressure vessel and these jumps are related to vibrations in the laboratory or other external events unrelated to the creep of the specimen.

The data shown in Figure 4 are very significant. The two experiments shown were performed at differential stresses of 131.0 MPa and 132.8 MPa. Only a partial section of the experiment performed at a differential stress of 131.0 MPa is shown; the specimen was subjected to a load for 732,000 seconds. In

ISSN 0148-9062

spite of the fact that the difference in the applied stress to each specimen is very small, 1.8 MPa, the rate of strain accumulation varies significantly. The specimen loaded to a differential stress of 132.8 MPa exhibits all three stages of creep. During the first 500 seconds of strain accumulation, the transient behavior is well displayed. The secondary creep, between 500 and 4500 seconds is quasi-linear. The strain accumulates at a more or less constant rate. The onset of tertiary creep at approximately 4500 seconds shows a rapidly accelerating strain rate resulting in failure of the specimen at an axial creep strain of 1.75 millistrain. The characteristics shown in these data are similar to those for the specimen tested at 134.6 MPa shown in Figure 3. The specimen tested at a differential stress of 131.0 MPa shows a much lower rate of strain accumulation. The total strain achieved during the transient creep is approximately half that of the specimen tested at 132.8 MPa. Furthermore, the rate of strain accumulation during secondary creep shown is much lower than that of the specimen tested at a differential stress of 132.8 MPa. Since both specimens were prepared from the same block of rock the sensitivity of the rate of strain accumulation to stress is very striking.

The sample tested at a differential stress of 127.8 MPa failed at 1.96×10^6 seconds. Due to a computer malfunction, the data after the onset of tertiary creep was lost. However, some acceleration in the rate of strain accumulation is observed prior to failure. The results of this experiment suggests that the onset of tertiary creep is precipitous for rocks subjected to differential loads for long times. Earlier constant strain rate experiments on the welded tuff from Busted Butte (Martin *et al*. 1993) showed that the magnitude of the dilatancy was much less than that observed on other low porosity crystalline rocks loaded to failure. More creep data on experiments failing at times greater than a million seconds are needed to test the universality of this observation.

All of the specimens tested showed a similar behavior. There was a pronounced transient primary creep followed by a continuous decrease in the rate of strain accumulation. For the specimens that failed, a tertiary creep was observed. For the specimens that did not fail, the rate of strain accumulation during secondary creep was low. In some cases, particularly in the specimens tested drained at a confining pressure of 10 MPa, and a temperature of 225 °C, the total creep was less than 0.4 millistrain. The data collected on the sixteen specimens are summarized in Table 1. The data include the porosity of the specimen, the state of stress, temperature, saturation, time to failure or, in cases where the specimens did not fail, the duration of the test, and the time dependent strain (creep strain) at which the specimen failed or the experiment was terminated.

There is some uncertainty in the stress at failure for the two specimens that failed in less than 5 seconds. Failure occurred during the loading phase of the experiment. The loading rate was high; it was difficult to precisely determine the stress at failure. All the specimens that failed, exhibited a definite shear plane. The fracture characteristics were similar to those observed in earlier experiments carried out in confined compression at a constant strain rate under identical conditions.

The suite of experiments carried out on specimens recovered from borehole NRG-7/7A showed very little strain accumulation, even for a test duration of 5.9×10^6 seconds. The strain accumulation during secondary creep is extremely small. For the specimens that failed, creep strains of greater than 2 millistrain were commonly observed. In contrast, for the experiments tested in drained condition at a higher temperature and a higher confining pressure the creep strain are all less than 0.4 millistrain.

DISCUSSION

The data collected on the creep experiments are consistent with a moisture assisted, time dependent crack

ISSN 0148-9062

growth mechanism. First, a comparison of the data for stable crack growth in single crystal quartz is similar to that observed in each of the creep experiments. With increasing stress the rate of crack growth increases. Presumably, when the cracks reach a critical length they interact and the specimen fails. The failure is preceded by tertiary creep. Comparing the data collected in Figures 3, 4, and 5, we see that as the stress is increased the strain rate increases and the time to failure decreases.

With the limited data set collected to date, it is not possible to consider the effects of the partial pressure of water and temperature on the rate of strain accumulation. Two conditions were explored at two temperatures, two confining pressures, and different water saturations. It is difficult to compare these data. First, the confining pressures for each suite of experiments is different. Second, all the samples tested from the NRG-7/7A borehole were not prepared from the same block of material. Therefore, material differences enter into any analysis.

Based on the studies of crack growth in single crystals, we expect that with increasing temperature, the creep rate will increase and time to failure at a fixed stress will decrease. Furthermore, since the specimens from Busted Butte were tested fully saturated they represent the most critical situation with respect to water saturation. If the partial pressure of water in the specimens is decreased, the creep rate will decrease and the time to the onset of tertiary creep will increase. Clearly, additional tests are necessary to clearly define these behaviors.

Previous experiments conducted on welded tuff corroborate time dependent stable cracking as a mechanism of deformation in welded tuff. Martin *et al*. 1993 observed a decrease in strength with decreasing strain rate for tuff from Busted Butte. The unconfined compressive strengths, for saturated specimens at room temperature, decreased nearly 28% for a thousand fold decrease in strain rate over the range from 10^{-5} to 10^{-9} s^{-1}. Similar effects have been reported by Charles 1959, and Obura *et al*. 1996. Martin *et al*. 1993 proposed that a constant strain rate experiment can be idealized as a series of incremental loading to successively higher stresses; the duration of the intervals increases with decreasing strain rate. At a constant load, the cracks propagate time dependently. The longer the time before augmenting the stress (that is, the longer the duration of the localized creep event), the more the cracks will extend prior to the next increment of the stress. Assuming that most rocks fail when cracks reach a critical length, the strengths of the rocks will decrease with increasing strain rate.

For brittle rocks, the strain at failure is extremely small (typically less than 0.5%) and varies by as much as a factor of two for nearly identical specimens. Furthermore, the creep strain accumulation is not linear with time. This makes estimation of the time to failure difficult to predict. For this reason, brittle rocks are often treated in terms of static fatigue. That is, the time to failure is plotted as a function of the applied stress. In this way, an estimate of the long term strength of the rocks and a measure of its uncertainty can be achieved without specific reference to the associated strain.

Six of the rocks from Busted Butte failed and are analyzed in terms of static fatigue. In Figure 6, the time to failure for each specimen is plotted as a function of differential stress. The specimens that did not fail are also included. From these data it is evident that as the differential stress on a specimen tested at 150 °C, a confining pressure of 5.0 MPa, and a pore pressure of 1.0 MPa, the time to failure increases with decreasing stress. There is scatter in the results. First, consider the two specimens that failed at times less than five seconds. There is some uncertainty as to the exact stress and the time to failure for these specimens. The uncertainty is due to the nature of the loading. The samples broke as the stress was increasing so rapidly that it is difficult to unravel the exact time to failure and the stress at failure from the

ISSN 0148-9062

stress and strain data. For experiments that failed at times greater than 100 seconds there is a clear tendency for small decreases in differential stress to produce large increases in the time to failure. For example, a specimen tested at 134 ± 0.2 MPa failed in several hundred seconds. At a differential stress of 128.7, the time to failure exceeded several million seconds. A measure of the scatter in these data is given by the two specimens tested at, 131.3 ± 0.1 MPa did not fail at times near a million seconds. A curve was fitted through the set of the six specimens that failed in creep. The time to failure is given by:

$$\langle t \rangle = 10^{41} e^{-0.646 \sigma} \qquad (5)$$

where $\langle t \rangle$ is the time to failure at a constant differential stress of σ. Given the limited data set, and the scatter, this expression will need to be reinforced with further experimentation. In spite of its limited range, the data shows that the time to failure is extremely sensitive to small changes in differential stress. For example, using Equation (5), a specimen loaded at a differential stress of 115 MPa will break after seventeen years. Furthermore, if we consider that the design life of the repository as ten thousand years, we find that a rock mass under similar boundary conditions, stressed to less than 105 MPa should not fail during that period. Given that the repository horizon will not be fully saturated as the temperature increases, we infer from Equation 1, that the time to failure at a given stress will increase with decreasing water concentration. Therefore, it appears that the static fatigue data shown in Figure 6 present a lower bound to the likelihood of failure of a rock mass subjected to a constant stress for extended periods of time.

While decreasing saturation of a rock subjected to a constant differential stress increases the time to failure, other factors influence the behavior of the repository. For example, Price 1986 studied the effect of sample size on the strength of welded tuff specimens recovered from Busted Butte. He observed that the compressive strength of the rock decreased as the volume of the sample increased. More than a 50% in reduction of strength was noted as the diameter of the test specimen was increased from 25 to 230 mm. Consequently, the effect of increasing scale will tend to reduce the strength, whereas drying the specimen will increase the time to failure dramatically. We are in a time, stress, temperature, moisture content, and scale continuum that must be mapped out to accurately predict the stability of the repository over its designed life. The static fatigue data presented above is a useful first step in the performance assessment of the repository. With additional data the long term stability of the repository can be modeled with greater confidence.

ACKNOWLEDGMENT

Portions of this work was performed under the auspices of the U.S. Department of Energy (DOE), Office of Civilian Radioactive Waste Management, Yucca Mountain Site Characterization Project, under Contract No. DEAC04-76DP900789 and Contract No. DE-AC04-94AL85000.

ISSN 0148-9062

FIGURES

Paper 190, Figure 1.

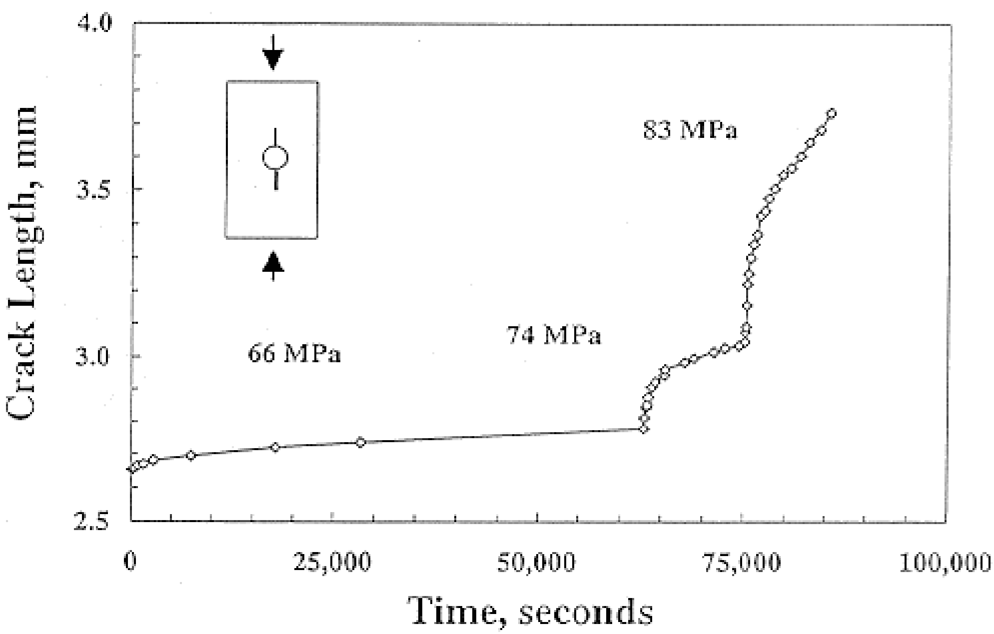

Figure 1. Crack length is shown as a function of time for an axial crack growth experiment in single crystal quartz. The experiment was conducted at a temperature of 241 °C and a partial pressure of water of 4.5×10^{-2} kPa (after Martin 1972).

ISSN 0148-9062

Paper 190, Figure 2.

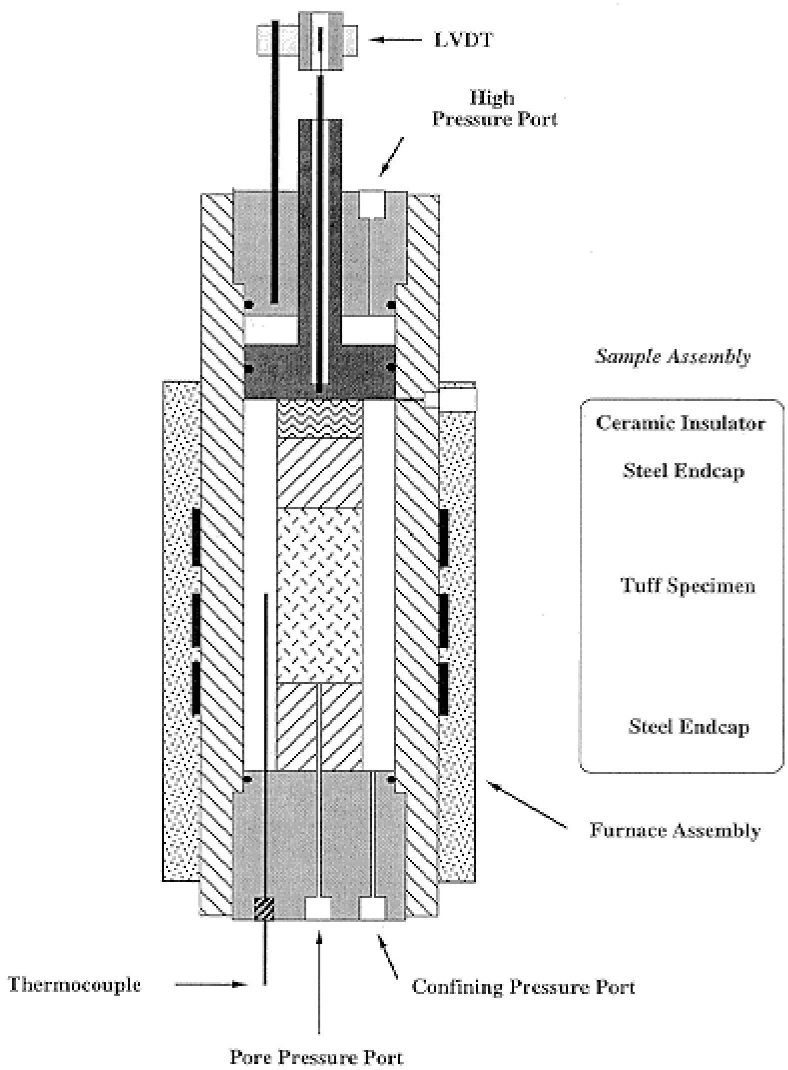

Figure 2. A schematic diagram of the test apparatus used in the creep and static fatigue tests at elevated temperatures.

ISSN 0148-9062

Paper 190, Figure 3.

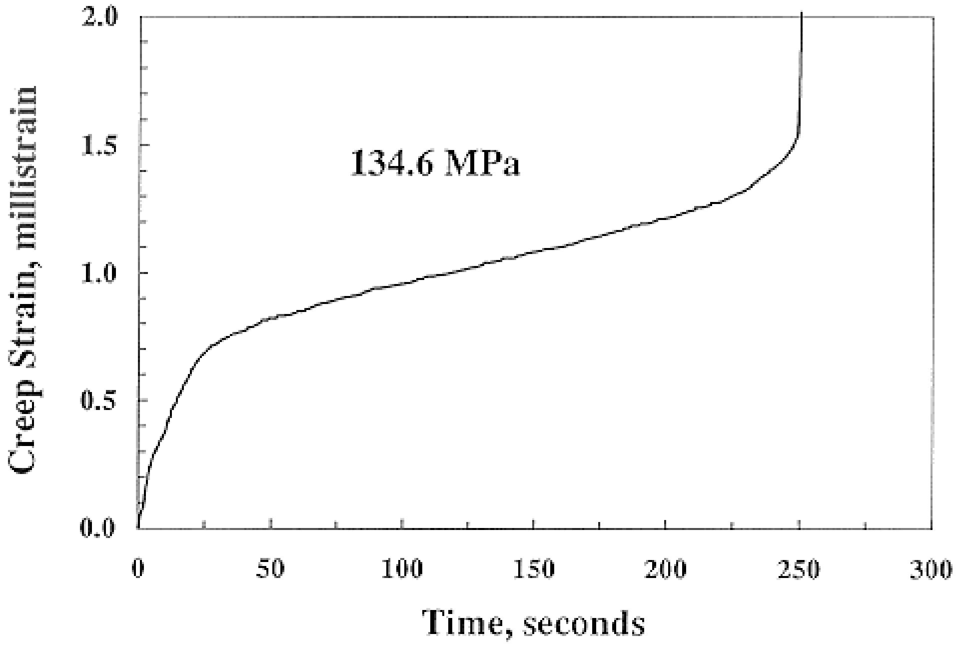

Figure 3. Creep strain is plotted as a function of time for an experiment conducted at a constant differential stress of 134.6 MPa, a confining pressure of 5.0 MPa, a pore pressure of 1.0 MPa, and a temperature of 150 °C. The specimen failed.

ISSN 0148-9062

Paper 190, Figure 4.

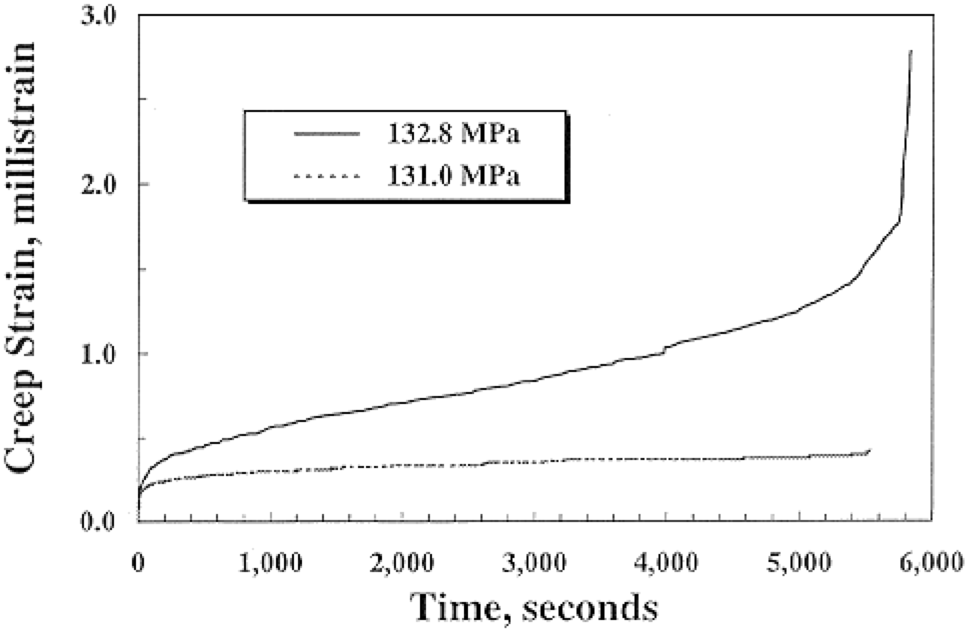

Figure 4. Creep strain is plotted as a function of time for two specimens. Both experiments were conducted at a confining pressure of 5.0 MPa, a pore water pressure of 1.0 MPa, and a temperature of 150 °C. One experiment was conducted at a differential stress of 132.8 MPa; the specimen failed. The data for the second experiment conducted at a differential stress of 131.0 MPa; only the initial portion of the experiment is shown.

ISSN 0148-9062

Paper 190, Figure 5.

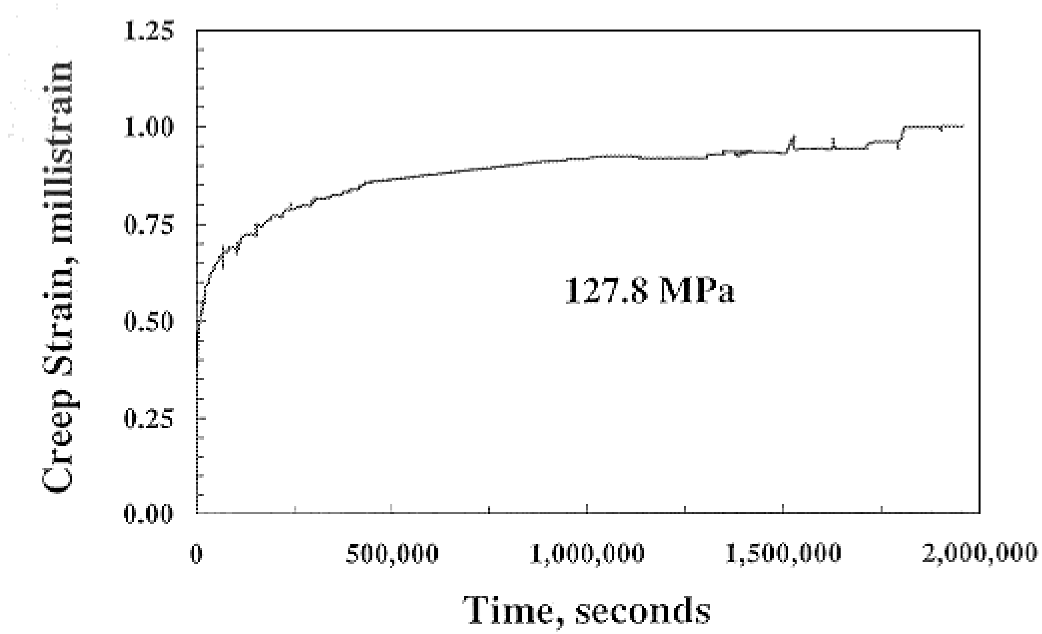

Figure 5. Creep strain is plotted as a function of time for an experiment conducted at a constant differential stress of 127.8 MPa, a confining pressure of 5.0 MPa, a pore pressure of 1.0 MPa, and a temperature of 150 °C. The experiment was terminated when the specimen failed.

ISSN 0148-9062

Paper 190, Figure 6.

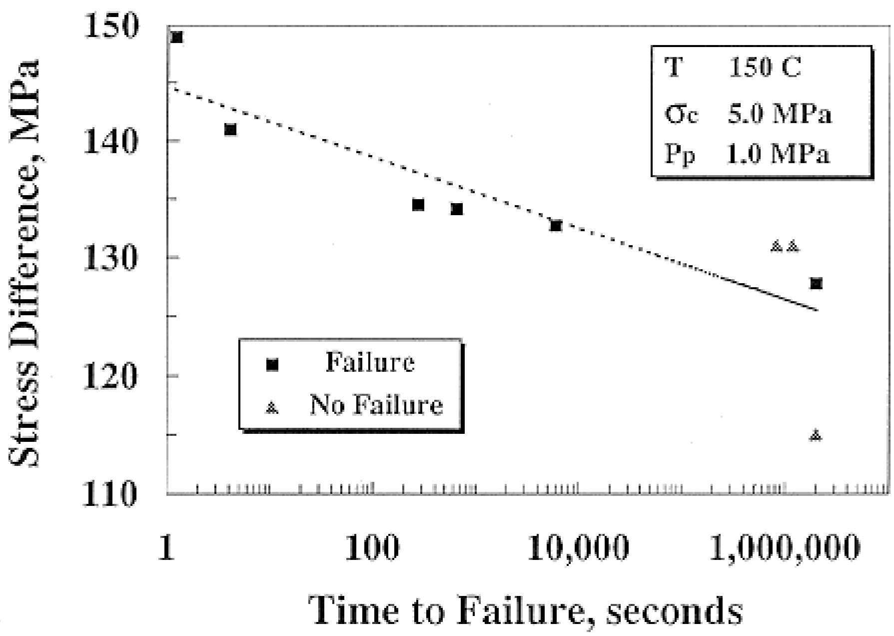

Figure 6. Stress difference is plotted as a function of time to failure for specimens of Busted Butte, welded tuff tested at a confining pressure of 5.0 MPa, a pore pressure of 1.0 MPa, and a temperature of 150 °C. Six specimens failed. The data for three experiments that were terminated prior to failure are also shown.

TABLES

ISSN 0148-9062

Paper 190, TABLE 1.

TABLE 1
CREEP SUMMARY

Specimen	Porosity %	Stress Difference, MPa	Confining Pressure, MPa	Pore Pressure, MPa	Temperature °C	Failure Time, (t), seconds	Creep Strain @ (t), millistrain
BB-9392-K	7.5 - 9.0	149 ± 10	5.0	1.0	150	1.2	3.0 ± 1.0
BB-9392-N	7.5 - 9.0	141 ± 4	5.0	1.0	150	4	3.0 ± 1.0
BB-9392-E	7.5 - 9.0	134.6	5.0	1.0	150	250	1.54
BB-9392-C	7.5 - 9.0	134.2	5.0	1.0	150	636	2.89
BB-9392-F	7.5 - 9.0	132.8	5.0	1.0	150	5,848	2.66
BB-9392-B	7.5 - 9.0	127.8	5.0	1.0	150	1,960,000	1.00
BB-9392-H	7.5 - 9.0	131.4	5.0	1.0	150	1,180,000 *	1.19
BB-9392-G	7.5 - 9.0	131.3	5.0	1.0	150	732,000 *	0.76
BB-9392-J	7.5 - 9.0	115.0	5.0	1.0	150	2,000,000 *	0.36
NRG 7-776.6	11.3	70.0	10.0	0	225	3,760,000 *	0.18
NRG 7-807.6	10.3	40.0	10.0	0	225	3,760,000 *	0.08
NRG 7-808.3	9.2	129.0	10.0	0	225	5,900,000 *	0.04
NRG 7-858.4	8.7	100.0	10.0	0	225	3,760,000 *	0.19
NRG 7-1264.5	11.4	98.0	10.0	0	225	2,550,000 *	0.24
NRG 7-1281.4	11.5	132.0	10.0	0	225	2,550,000 *	0.34
NRG 7-1400.5	8.8	131.0	10.0	0	225	2,550,000 *	0.37

References

References

Atkinson B. K. 1984. Subcritical crack growth in geological materials. *J. Geophys. Res.*, **89**, 4077–4114.

Brace W.F., B.W.Paulding Jr. , C.H.Scholz 1966. Dilatancy in the fracture of crystalline rocks. *J. Geophys. Res.*, **71**, 3939–3953.

Charles R.J. 1965. The strength of silicate glasses and some crystalline oxides, high strength materials. John Wiley, New York.

Dunning J. D., W.L.Lewis , D.E.Dunn 1980. Chemomechanical weakening in the presence of surfactants. *J. Geophys. Res.*, **85**, 5344–5354.

Hardy M. P, S. J.Bauer 1992. Rock mechanics considerations in designing a nuclear waste repository in hard rock. *Rock Mechanics Proceedings of the 33rd U.S. Symposium.* A.A. Balkema, ed. by J.R. Tillerson & W.R. Wawersik, 1041.

Kranz R. L., C.H.Scholz 1977. Critical dilatant volume of rocks at the onset of tertiary creep. *J. Geophys. Res.*, **82**, 4893–4898.

ISSN 0148-9062

Lomnitz C. 1956. Creep measurements in igneous rocks. *J. Geol.,* **64**, 473–479.

Martin R.J.III 1972a. Time-dependent crack growth in quartz and its application to the creep of rocks," *J. Geophys. Res.,* **77**, 1406.

Martin R.J.III 1972b. Static fatigue and creep of quartzite. *Eos Trans.,* AGU, **53:4**, 515.

Martin R.J.III , W.B.Durham 1975. Mechanisms of crack growth in quartz. *J. Geophys. Res.,* **80**, 4837.

Martin R.J.III , R.H.Price , P.J.Boyd , J. S.Noel 1993. The influence of strain rate and sample inhomogeneity on the moduli and strength of welded tuff. *Int. J. Rock Mech. Min. Sci. & Geomech. Abstr.* **15:7**, 1507–1510.

Matsushima S. 1960. On the flow and fracture of igneous rocks. *Disaster Prevention Res. Inst., Kyoto Univ. Bull,* **36**, 2–9.

Obura Y., K.Sugawara , N.Tokashiki 1996. Influence of water vapor pressure on strength of rocks in uniaxial compression. Proceedings of the 2nd North American Rock Mechanics Symposium: NARMS '96, ed. Aukertin, Hassani, and Mitri, **2**, 1337–1342.

Peng Syh-Deng 1973. Time-dependent aspects of rock behavior as measured by a servocontrolled hydraulic testing machine. *Int. J. Rock Mech. Min. Sci. & Geomech. Abstr.* **10**, 235–246.

Price R.H. 1986. Effects of sample size on the mechanical behavior of topopah spring tuff. SAND850709, Sandia National Laboratories.

Rummel F. 1969. Studies of time-dependent deformation of some granite and eclogite samples under uniaxial, constant compressive stress and temperatures up to 400° C. *J. Geophys.,* **35**, 17–42.

Scholz C.H. 1968. Mechanism of creep in brittle rock. *J. Geophys. Res.,* **73**, 3295.

Scholz C.H. 1972. Static fatigue of quartz. *J. Geophys. Res.,* **77:11**, 2104, 1972.

Wawersik W.R. 1972. Time-dependent rock behavior in uniaxial compression. *Proceedings of the 14th Symposium on Rock Mechanics.* 85–106, Pennsylvania State University, University Park, PA.

Wiederhorn S. M. 1968. Moisture assisted crack growth in ceramics. *Int. J. Fracture Mech,* **4:2**, 171–177.

ISSN 0148-9062